

UNCLASSIFIED

Defense Technical Information Center  
Compilation Part Notice

ADP011034

TITLE: Direct Synthesis of Silicon Nanowires, Silica Nanospheres, Wire-Like Nanosphere Agglomerates, and Silica-Based Nanotubes and Nanofiber Arrays

DISTRIBUTION: Approved for public release, distribution unlimited

This paper is part of the following report:

TITLE: Materials Research Society Symposium Proceedings Volume 635. Anisotropic Nanoparticles - Synthesis, Characterization and Applications

To order the complete compilation report, use: ADA395000

The component part is provided here to allow users access to individually authored sections of proceedings, annals, symposia, etc. However, the component should be considered within the context of the overall compilation report and not as a stand-alone technical report.

The following component part numbers comprise the compilation report:

ADP011010 thru ADP011040

UNCLASSIFIED

**Direct Synthesis of Silicon Nanowires, Silica Nanospheres, Wire-Like Nanosphere Agglomerates, and Silica-Based Nanotubes and Nanofiber Arrays**

**J. L. Gole,<sup>1</sup> J. D. Stout,<sup>1</sup> Z. R. Dai,<sup>2</sup> and Z. L. Wang<sup>2</sup>**

Schools of Physics,<sup>1</sup> and Material Science<sup>2</sup>

Georgia Institute of Technology, Atlanta, Georgia 30332-0430

(ph294jg@prism.gatech.edu, 404-894-4029)

For several decades, the vapor-liquid-solid (VLS) process,<sup>1,2</sup> where gold particles act as a mediating solvent on a silicon substrate, forming a molten alloy, has been applied to the generation of silicon whiskers. The diameter of the whisker is established by the diameter of the liquid alloy droplet at its tip. The VLS reaction generally leads to the growth of silicon whiskers epitaxially in the  $\langle 111 \rangle$  direction on single crystal silicon  $\langle 111 \rangle$  substrates.<sup>1-3</sup> Recently, Lieber,<sup>4</sup> Lee,<sup>5</sup> Yu,<sup>6</sup> and coworkers have extrapolated on the ideas entailed in the VLS technique to develop laser ablation of metal containing silicon targets, obtaining bulk quantities of silicon nanowires. More recently, Lee et al.<sup>5,7</sup> have shown that oxides play a dominant role in the nucleation and growth of semiconductor nanowires be it by laser ablation, thermal evaporation, or chemical vapor deposition. Lee et al.<sup>5</sup> have suggested a new growth mechanism, referred to as oxide assisted nanowire growth, which represents a new approach to nanowire synthesis. Our initial approach<sup>8-10</sup> to this problem has involved the application of the techniques of high temperature synthesis to modify the approach of Lee et al. and generate virtually defect free  $\text{SiO}_2$  sheathed crystalline silicon nanowires and silica ( $\text{SiO}_2$ ) nanospheres which can be agglomerated to wire-like configurations impregnated with crystalline silicon nanoclusters. Further controlled condensation can extend this agglomeration to produce nanotubes and nanofiber arrays.

Figures 1 correspond to Transmission Electron Micrographs of exemplary virtually uniform and straight nanowires which we have generated from a 50/50 Si/ $\text{SiO}_2$  equimolar mixture heated to a temperature of 1400°C at a total pressure of 225 Torr for 12 hours. The central crystalline silicon core is  $\sim 30$  nm in diameter whereas the outer  $\text{SiO}_2$  sheathing is  $\sim 15$  nm in thickness. The HRTEM views in Figures 1(b) and (c) demonstrate a number of distinguishing characteristics. Figure 1(c) demonstrates that the axes of the  $\text{SiO}_2$  clad crystalline silicon nanowires are parallel to  $\langle 111 \rangle$ . This is distinct from the results obtained by Lee et al.<sup>5</sup>

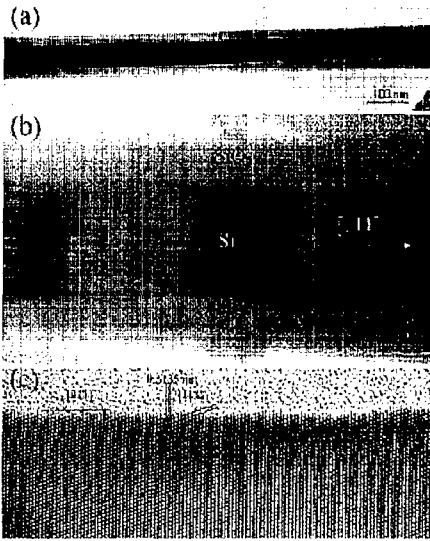


**Fig 1**

TEM of (a) SiO<sub>2</sub> sheathed crystalline nanowire, (b) closer view showing (1) slight undulations and stress patterns which are apparent in a virtually defect free nanowire, and (c) closer view showing crystalline core axes parallel to  $\langle 111 \rangle$  direction. Synthesized @ 1400C from 50/50 Si/SiO<sub>2</sub> mix (P<sub>total</sub> = 225 Torr, flow rate 100 sccm of UHP argon).

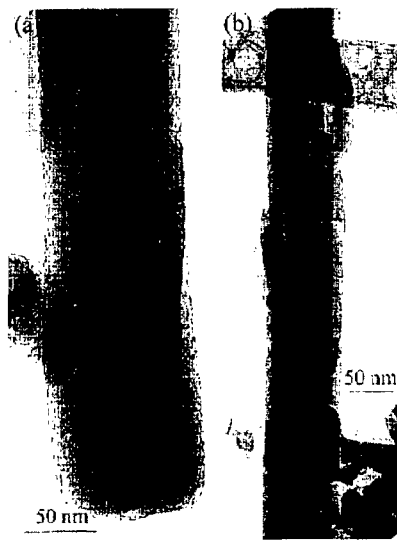


**Fig 2**

TEM closeup view of (a) end of SiO<sub>2</sub> sheathed crystalline silicon nanowire showing pinch off of inner crystalline core at the end of the formation process and (b) opposite end of SiO<sub>2</sub> sheathed crystalline silicon wire showing strength of SiO<sub>2</sub> sheath. Conditions as in Fig 1.

whose wires have their axes parallel to  $\langle 112 \rangle$  as they display twinning, high order grain boundaries, and stacking faults. At the Si-SiO<sub>2</sub> interface, (Fig. 1(c)), the crystal planes are best described as  $\{211\}$ . The wire which is depicted in Figures 1 appears virtually defect free. As figure 1(b) suggests, the inner crystalline silicon core undulates slightly. However, the fluctuations in the shading that are apparent in the HRTEM micrograph indicate that the wires are of sufficient quality that the detailed strain due to slight bending above the TEM mount can be readily observed in the micrograph.

Figures 2(a) and 2(b) demonstrate further distinguishing characteristics of the nanowires which we have generated. Figure 2(a) demonstrates the pinch off of the crystalline silicon core at the beginning of the wire growth, suggesting a distinctly different formation mechanism than that suggested by Lee et al.<sup>5</sup> for their wires generated using a similar source and by Morales and Lieber<sup>2</sup> for their iron catalyzed wire formation from Fe/Si mixtures generated using laser ablation. While Lee et al.<sup>5</sup> find evidence for a growth mechanism along  $\langle 112 \rangle$  with which they associate a complex process involving Si<sub>3</sub>O formation, the observed structure in Figure 2(a) would suggest at least a close analogy to the VLS mechanism, albeit with an apparent self assembly of the silicon in the absence of a metal catalyst. Further, the data in Figure 2(b), which shows the opposite end of the same nanowire suggests a significant strength for the outer SiO<sub>2</sub> sheath. Finally, a comparison to the TEM micrographs of Lieber et al.,<sup>4</sup> which show the clear termination of their nanowires at larger - nearly spherical FeSi<sub>2</sub> nanoclusters, offers yet an additional contrast, suggesting that there are a number of potential approaches to nanowire synthesis.

Figure 3 corresponds to an exemplary TEM micrograph of dispersed silica (SiO<sub>2</sub>) nanospheres of diameter  $\approx 30$  nm which can be generated in gram quantities (Figure 4) on a cold plate placed in the gas flow field of our high temperature synthesis source. As a function of slightly modified experimental conditions,<sup>11</sup> these nanospheres have a nearly monodisperse particle size distribution and vary in size from  $\approx 45$  to 8 nm in diameter. Transmission Electron Microscopy, TEM,<sup>8</sup> X-ray diffraction,<sup>8</sup> and ESR<sup>12</sup> measurements now demonstrate that the nanospheres are amorphous and absent of dangling bonds. They have been used to sequester active copper sites for the selective conversion of ethanol to acetaldehyde<sup>13</sup> in a process that is at least three times more effective than that using fumed silica produced from the flame hydrolysis of silicon tetrachloride.<sup>14</sup> Further, it has been possible to reduce a Ni(III) solution in an

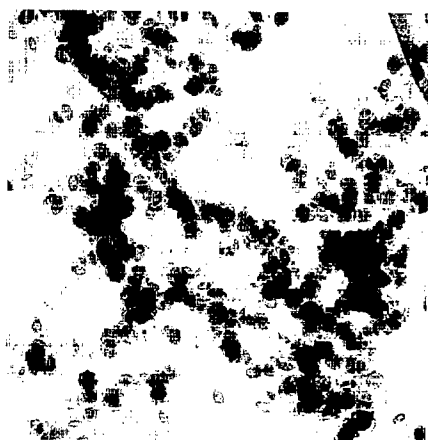


**Fig 3**  
TEM of virtually "monodisperse" SiO<sub>2</sub> nanospheres 30nm in diameter.



**Fig 4**



**Fig 5**  
TEM micrographs of (a) SiO<sub>2</sub> nanospheres agglomerating into wire-like groupings and (b) closer view showing crystalline silicon nanoclusters (see diffraction pattern insert) impregnating the SiO<sub>2</sub> wire-like agglomeration.

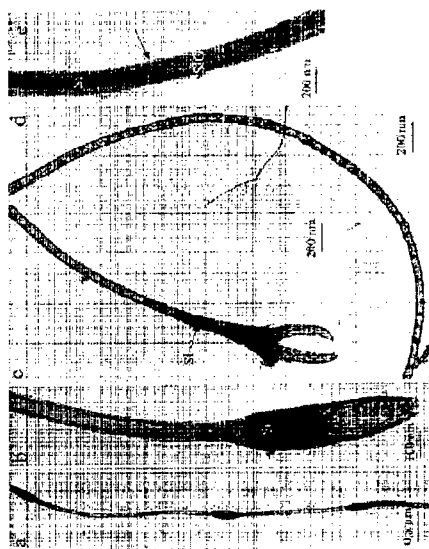
electroless process on the surface of the nanospheres, producing a ferromagnetic crystalline nickel coating<sup>12</sup> of variable thickness.

With additional adjustments of flow rates and temperature gradients, it is possible to agglomerate the nanospheres into the wire-like configurations depicted in Figure 5 (a) which, on closer view, correspond to wire-like SiO<sub>2</sub> nanosphere agglomerates impregnated by crystalline silicon nanoclusters (Figure 5 (b) and inset). This agglomeration can be extended in a controlled manner to produce the variety of silica nanotubes and nanofiber arrays depicted in Figures 6 and 7.

The initiation of nanotube growth appears to involve seeding by crystalline silicon particles along the growth direction. Figure 6(a) depicts the growth of the silica nanotubes between crystalline silicon particles which may also impregnate the tubes. The image displayed in Figure 6(b) suggests that a silicon particle is located at the area that links aligned nanofiber arrays, similar to those also depicted in Figure 7, and a silica nanotube. The outer diameter of the tubes is

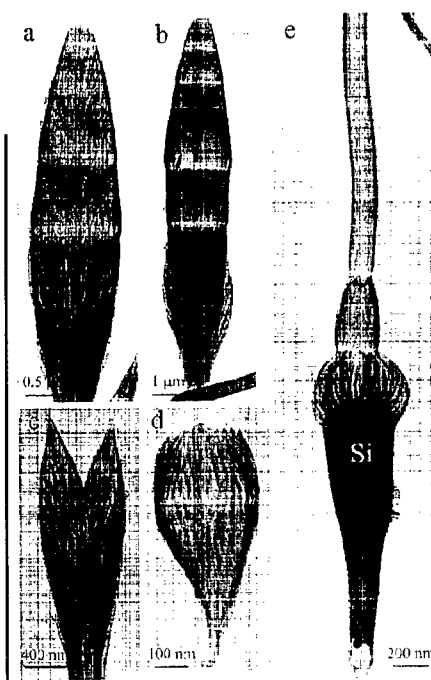
1 70-80 nm, and the wall thickness is 1 20 nm. Thus, with their 30 nm inner-tube diameter, they would appear to be ideally suited for catalysis of high molecular weight hydrocarbons. It appears that the crystalline silicon particle blocks and hence terminates the growth of the silica nanofibers located inside the bundle, while the outermost fibers continuously grow in an oxidation process forming a continuous shell, which constitutes the nanotube. This process is also suggested by the structure shown in Figure 6(c), where the formation of a crystalline silicon particle at the end of a silica fiber agglomeration again appears to play a key role in the formation of the nanotube. In Figure 6(d) we demonstrate that the silica tubular structure can also display a "necklace-like" internal chain structure. This chain-like structure represents an intermediate between densely packed and aligned nanofibers and the continuous nanotube.

Figure 7 demonstrates an intriguing coalescence of silica nanowires to form a variety of unique three-dimensional structures. Shown in Figures 7(a-d) are typical cage structures composed of aligned silica nanofibers. The nanofibers grow into bundles, while paralleling a structure that has near cylindrical symmetry.<sup>9</sup> The width of the cage is 0.3 - 1  $\mu$ m much larger than the diameter of the silica nanofibers (ex. 1 20 nm). These arrays clearly demonstrate a significant versatility to those silica nanostructures which can be synthesized. In fact, Figure



**Fig 6**

TEM images of synthesized silica nanotube structures usually formed following the trapping of nanocrystals.

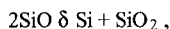
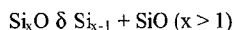


**Fig 7**

TEM images of silica "bundled" arrays and cages.

7(e) takes the shape of a “Chinese lantern” structure composed of silicon and  $\text{SiO}_x$ , where an  $\text{SiO}_x$  nanotube extends from the top of a silica wire bundle.

The direct synthesis results which we have obtained in concert with the results of Lee et al.<sup>5</sup> and Lieber et al.<sup>4</sup> would suggest that there are several exciting possibilities for the synthesis of useful silicon and silica based nanowires and nanostructures. Within our approach, we have modified and extended a configuration similar to that reported by Lee et al.<sup>5</sup> to generate the  $\text{SiO}_2$  passivated (sheathed) crystalline silicon nanowires using an Si-SiO<sub>2</sub> mix with further extensions to form nanotubes and nanofiber arrays. While Lee et al.<sup>9</sup> have noted that their approach produces silicon nanoparticles which they suggest subsequently form passivated nanowires via the combined steps



our results indicate that the judicious manipulation of this high temperature system including mixture stoichiometry, flow conditions (kinetics), and temperature range, yields more than would have been previously anticipated. In fact we have also used a carbon/SiO mixture to synthesize biaxial and coaxial SiC/SiO<sub>2</sub> nanowires.<sup>10</sup> The current results would seem to suggest that additional mechanisms may be operative which are analogs not only of a nanoscale VLS mechanism<sup>1-3</sup> but also involve a form of crystalline silicon as well as silica self assembly.



## References

1. G. A. Boostma and H. J. Gassen, *J. Cryst. Growth* **10**, 223 (1971).
- 1.A. M. Morales and C. M. Lieber, *Science* **279**, 208 (1998).
- 2.Y. F. Zhang, Y. H. Zhang, N. Wang, D. P. Yu, C. S. Lee, I. Bello, and S. T. Lee, *Appl. Phys. Lett.* **72**, 1835 (1998).
3. See for example, J. Hu, T. W. Odom, and C. M. Lieber, *Acc. Chem. Res.* **32**, 435 (1999) and references therein.
4. See for example, S. T. Lee, N. Wang, Y. F. Zhang, and Y. H. Tang, "Semiconductor Nanowires from Oxide", *MRS Bulletin*, August 1999, pg. 36, and references therein.
- 1.D. P. Yu, Z. G. Bai, Y. Ding, Q. L. Hang, H. Z. Zhang, J. J. Wang, Y. H. Zou, W. Qian, G. C. Xiong, H. T. Zhou, and S. Q. Feng, *Appl. Phys. Lett.* **72**, 3458 (1998).
- 1.N. Wang, Y. H. Tang, Y. F. Zhang, C. S. Lee, I. Bello, and S. T. Lee, *Chem. Phys. Lett.* **299**, 237 (1999).
- 1.J. L. Gole, J. D. Stout, W. L. Rauch, and Z. L. Wang, *Appl. Phys. Lett.* **76**, 2346 (2000).
- 2.R. P. Gao, Z. L. Wang, J. D. Stout, and J. L. Gole, *Advanced Materials* **12**, 1938 (2000).
- 3.Z. L. Wang, Z. R. Dai, Z. G. Bai, R. P. Gao, and J. L. Gole, *Appl. Phys. Lett.* **77**, 3349 (2000).
- 4.J. L. Gole, J. D. Stout, and Z. L. Wang, to be published.
- 5.S. M. Prokes, W. E. Carlos, Lenward Seals, Stephen Lewis, and James L. Gole, "Ferromagnetic Nickel Coated Silica Nanospheres from Electroless Solution", in preparation.
- 6.J. L. Gole and M. G. White, "New Cu/SiO<sub>2</sub> Based Catalyst for Selective Ethanol - Acetaldehyde Conversions", Georgia Tech invention disclosure, March 2000. "Nanocatalysis: Selective Conversion of Ethanol to Acetaldehyde Using Monoatomically Dispersed Copper on Silica Nanospheres", *Journal of Catalysis*, submitted.
- 7.Sales literature, Cabot Corporation.

## **Nanoparticles in Biology**